Sustainable Chemistry and Pharmacy 39 (2024) 101559

Contents lists available at ScienceDirect

Sustainable Chemistry and Pharmacy

journal homepage: www.elsevier.com/locate/scp

Biodiesel production using heterogeneous catalyst derived from natural calcite stone: Study of the effect of Mg–Zr doping and reaction conditions

Morteza Talebi [a], Afsanehsadat Larimi [b,**], Farhad Khorasheh [a], Tohid N. Borhani [c,*]

[a] Department of Chemical and Petroleum Engineering, Sharif University of Technology, Tehran, Iran
[b] Department of Chemical and Process Engineering, Niroo Research Institute, Tehran, Iran
[c] Center for Engineering Innovation and Research, School of Engineering Computing and Mathematical Sciences, University of Wolverhampton, WV1 1LY, UK

ARTICLE INFO

Handling Editor: Fabio Aricò

Keywords:
Transesterification
Calcite
Biodiesel
Canola oil
Magnesium
Zirconium

ABSTRACT

The aim of this study is to examine the impact of doping Mg–Zr on CaO derived from natural calcite, which are utilized as heterogeneous catalysts to produce biodiesel through the transesterification reaction of canola oil and methanol. The catalysts were synthesized via the wet impregnation method with varying concentrations of Mg–Zr (2.5, 5, 7.5, and 10 wt%) over the calcite, (Mg/Zr mass ratio of 2:1), followed by calcination at 600 °C. Physicochemical analyses, encompassing XRD, BET, SEM, EDX, and TGA, were employed for catalyst characterization. The samples' basicity was determined through titration. Operational parameters, including catalyst loading, methanol-to-oil ratio, reaction time, and temperature, were systematically explored. The stability and reusability of the optimal catalyst were also assessed. With the increase in the mass ratio of Mg–Zr to CaO, the total number of base sites on the catalyst increases, and maximum is achieved for the 7.5%(Mg–Zr)/CaO catalyst compared to other catalysts. Also observed a similar pattern in the variation of biodiesel yield, indicating a strong correlation between catalytic activity and the overall number of basic sites present on the catalyst surface. Results indicated that, under specific conditions (7 wt% catalyst loading, a methanol-to-oil molar ratio of 12:1, and a reaction temperature of 60 °C for a 3-h duration), the highest content of fatty acid methyl esters (FAME) reached 96.7% over on 7.5%Mg–Zr/CaO. The optimum catalyst exhibited robust stability and reusability across four consecutive reaction cycles, with the produced biodiesel meeting the standards of EN 14214 and ASTM D6751.

1. Introduction

The increase in global population and rapid economic growth has intensified the worldwide demand for energy. Unfortunately, a substantial portion of the world's energy resources is non-renewable (Larimi and Alavi, 2012). These resources, being finite, are on a trajectory toward depletion in the foreseeable future. Moreover, the combustion of these non-renewable fuels releases substantial volumes of greenhouse gases into the atmosphere, contributing significantly to the acceleration of climate change (Akbari et al., 2022). To effectively address global warming, a dual-pronged approach is imperative-embracing the adoption of renewable energies and the

* Corresponding author.
** Corresponding author.
E-mail addresses: alarimi@nri.ac.ir (A. Larimi), T.borhani@wlv.ac.uk (T.N. Borhani).

https://doi.org/10.1016/j.scp.2024.101559
Received 14 December 2023; Received in revised form 15 March 2024; Accepted 27 March 2024
Available online 10 April 2024

implementation of carbon capture, utilization, and storage (CCUS). Consequently, the prevailing trajectory is driving towards the substitution of fossil fuels with renewable alternatives, and biodiesel stands out prominently among these sustainable options (Koh and Ghazi, 2011).

Different types of renewable fuels are proposed in recent years (Sharifzadeh et al., 2019; Ezzatzadegan et al., 2021). Biodiesel is a renewable, biodegradable fuel manufactured from triglycerides. The major sources of triglycerides that are used as feedstock for the production of biodiesel are a variety of vegetable oils (edible (Saikia et al., 2023; Yusuff, 2021; Sronsri et al., 2021) and non-edible (Thakkar et al., 2022; Devarajan et al., 2022)), waste cooking oils (Elnasr et al., 2024) and animal fats (Moonsin et al., 2023; Salaheldeen et al., 2021). This fuel has physicochemical features similar to diesel obtained from a crude oil refinery and could be used directly or as a mixture with fossil-based diesel without requiring a change in the diesel engines (Helwani et al., 2009). It is non-toxic, biodegradable, and produces less pollution than the combustion of fossil fuels.

Transesterification is the most feasible way to turn triglycerides into biodiesel that has similar viscosities to diesel fuel. The most common method of transesterification is the reaction of the ester with an alcohol (methanol or ethanol) in the presence of a catalyst (Maleki et al., 2017). The catalysts used in the transesterification reaction are either heterogeneous or homogeneous (Kaur and Ali, 2011). Homogeneous basic catalysts (e.g. NaOH (Roschat et al., 2024) and KOH (Suherman et al., 2023)) are more commonly used than homogeneous acid catalysts (e.g. HCl and H_2SO_4) in the transesterification reaction due to their high activity requiring shorter reaction time and more moderate operating conditions (Lam et al., 2010). Homogeneous acidic or basic catalysts have some shortcomings as they cause corrosion, are sensitive to the amount of free fatty acids, and pose difficulty in separation from the products thereby increasing the final price of biodiesel produced (de Lima et al., 2016). In order to solve these problems, heterogeneous catalysts have been proposed. It must be mentioned that solid basic heterogeneous catalysts are more widely used compared with solid acidic catalysts because they require lower operating temperatures and shorter reaction times (Kaur and Ali, 2014). Different types of basic heterogeneous catalysts used for biodiesel production have been investigated including alkali oxides, alkaline earth oxides, and mixed metal oxides (Tahvildari et al., 2015; Roschat et al., 2022; Chen et al., 2015a; Sree et al., 2009; Ahmadkhani et al., 2019; Dahdah et al., 2021). Among the various solid basic catalysts, calcium oxide (CaO) is one of the most highly active catalysts in the transesterification reaction. This catalyst is also most widely used due to its low cost, availability, lower solubility in the reaction products, and efficient recovery (Ahmadkhani et al., 2019). CaO is also used as a catalyst support due to its large surface area and high porosity. Calcium oxide is a non-toxic catalyst with sufficient basicity to enhance biodiesel production (Kaur and Ali, 2011).

To reduce the cost of biodiesel production, many investigations have focused on the use of cheap and readily available sources of calcium including industrial waste sources [e.g. lime mud (Nabgan et al., 2022), constructional lime (Ghanei et al., 2013), red mud (Ba et al., 2022)), biological wastes (e.g. shells (Roschat et al., 2020), mollusk shells (Phewphong et al., 2022), bones (Babatunde et al., 2022) and natural sources (e.g. dolomitic rock (Ali et al., 2022), lime (Weldeslase et al., 2023), clays and calcite (Payapo et al., 2023; Widiarti et al., 2019)).

Mahesh et al. (2015) noted solid base catalysts such as CaO can experience a decline in activity due to the adsorption of CO_2 and H_2O from the atmosphere. This phenomenon leads to the poisoning of base sites on the catalyst surface and alters the crystal structure of the solid catalyst. Pure CaO exhibits sensitivity not only to free fatty acids (FFA) and moisture but also demonstrates partial solubility in alcohol and glycerol. Furthermore, a significant amount of research has been conducted to modify CaO with the aim of enhancing its stability and catalytic activity. In order to modify, the impregnation of an active catalytic precursor or combining with alkaline and alkaline earth oxides can be used (La Ore et al., 2020). Kaur and Ali (2014) conducted the synthesis of various concentrations of Zr on CaO using the wet impregnation method and calcined them up to 900 °C. Subsequently, these catalysts were utilized in the transesterification reaction of Jatropha oil with methanol. Their study findings suggest that 15%Zr/CaO (calcined at 700 °C) demonstrated the highest catalytic activity compared to all other prepared catalysts, including pure CaO. Xia et al. (2014) synthesized CaO–ZrO_2 catalysts with various Ca/Zr ratios ranging from 4/6 to 9/1 employing the urea/nitrate combustion method. Subsequently, these prepared catalysts were applied in the transesterification reaction of soybean oil with methanol to produce biodiesel. As the Ca/Zr ratio increased, the total number of active sites also increased, reaching its maximum for the CaO–ZrO_2 catalyst

Table 1
Modified resources of waste and natural material to produce biodiesel.

Catalyst	Feedstock	Reaction conditions (Catalyst dosage, methanol to oil ratio, Temperature, and reaction time)	Yield*/ Conversion**	Ref.
KOH/Bentonite	Palm oil	3 wt%, 6:1, 60 °C , 3 h	90.7*	Soetaredjo et al. (2011)
H_2SO_4/sea sand	Safflower oil	7.5 wt%, 12:1, 60 °C , 6 h	96.6*	Muciño et al. (2014)
KF/lime mud	Peanut oil	5 wt%, 12:1, 64 °C , 5 h	99**	Li et al. (2014)
Constructional lime	Waste frying oil	1 wt%, 12:1, 65 °C , 2 h	93.9**	Ghanei et al. (2013)
Li/egg shell	Nahor oil	5 wt%, 10:1, 65 °C , 4 h	94**	Boro et al. (2014)
CaO–CeO_2/chicken bone	Refined palm oil	11 wt%, 9:1, 65 °C , 3 h	91.8*	Yan et al. (2016)
KI/oyster shell	Soybean oil	1 mol/g, 10:1, 50 °C , 4 h	79.5**	Jairam et al. (2012)
MgO–ZrO_2/calcite	Canola oil	7 wt%, 12:1, 60 °C , 3 h	96.8*	This study

with a Ca/Zr ratio of 8/2. A similar correlation was also observed in the biodiesel production process. Hu et al. (2023) synthesized MgO–CaO catalysts with varying Mg/Ca molar ratios (0:1, 1:3, 2:3, 1:1, and 1:0) using the co-precipitation method, which were subsequently utilized in the transesterification reaction of palm oil with methanol to produce biodiesel. Their findings highlighted that the incorporation of Mg led to a reduction in the CaO lattice spacing, enhancement of sensitivity, and an increase in the number of active sites, thereby resulting in improved catalyst activity. Notably, the $1Mg_3Ca$ (Mg/Ca = 1/3) catalyst exhibited the highest catalytic activity, achieving 92% yield biodiesel at a reaction temperature of 60 °C over a duration of 2 h. Moulai et al. synthesized Mg–Zr mixed oxide with different molar ratios of Ca to Zr as a heterogeneous catalyst and analysed its performance in the transesterification reaction of waste cooking oil with ethanol. The addition of Zr to Ca resulted in the formation of active crystals of $CaZrO_3$, which exhibited high efficiency. Under the optimum reaction conditions of a 10 wt% catalyst loading, a methanol-to-oil molar ratio of 30:1, and a reaction temperature of 65 °C for a 2-h duration, the Mg–Zr catalyst with a molar ratio of approximately 0.5 Ca to Zr showed the highest yield of 93% (Dehkordi and Ghasemi, 2012). Table 1 briefed some studies on the production of biodiesel from these sources.

Considering the mentioned issues related to CaO sensitivity and solubility in glycerol and methanol, the focus of the current study is on increasing stability and catalytic activity of CaO derived from natural calcite. For the first time, our study involved doping different concentrations of the Mg–Zr combination onto calcined calcite using the wet impregnation method. It has also been reported that the combination of Mg–Zr with a weight ratio of Mg/Zr = 2 has shown very good activity and stability in the transesterification reaction of biodiesel production (Sree et al., 2009; Li et al., 2011). The performance of Mg–Zr and their activity catalysts supported on CaO is investigated in this study in the transesterification reaction to produce low-cost biodiesel. BET, X-ray diffraction (XRD), Thermogravimetric analysis (TGA), and Scanning electron microscopy (SEM) characterizations were used to investigate the physical/chemical properties of the synthesized catalysts. The effects of experimental parameters (catalyst loading, methanol/oil molar ratio, reaction temperature, and reaction time) as well as the stability of the optimum catalyst were examined. Canola oil was chosen as the feedstock due to its high oil content and relatively low saturated fat levels compared to other major vegetable oils. These characteristics contribute to the enhanced performance of its biodiesel product, particularly in cold weather conditions. Additionally, biodiesel derived from canola oil is recognized as a viable alternative fuel for combustion in diesel engines, as it can be utilized without requiring significant engine modifications.

2. Materials and methods

2.1. Materials

Canola oil was purchased from a local store (Tehran, Iran) and its physico-chemical characteristics are presented in Table 2. Calcite stones were obtained from the Aligudarz mine in Iran. Methanol (99%), $Mg(NO_3)_2$, $ZrOCl_2{\cdot}8H_2O$, benzene, benzoic acid, and bromothymol blue were purchased from Merck.

2.2. Catalyst preparation

As shown in Fig. 1, the calcite stones were first crushed using an agate mortar and then sieved to obtain the desired powder size (100 mesh). The calcite powder was subsequently calcined at 800 and 900°C for 4 h using a muffle furnace. After cooling, the calcined calcite powder was stored in a closed vessel to avoid contact with carbon dioxide and atmospheric moisture. The Mg–Zr/CaO catalysts were prepared by wet impregnation. To prepare a 5% Mg–Zr/CaO catalyst, 1.4 g of $Mg(NO_3)_2$ and 0.23 g of $ZrOCl_2{\cdot}8H_2O$ were dissolved in 50 ml distilled water. The solution was subsequently added to 3.8 g of calcined calcite powder and allowed to mix by a magnetic stirrer at room temperature for 4 h. The resulting slurry was dried at 110°C for 12 h and then calcined at 600°C for 4 h. The obtained catalysts were labelled as *y*Mg-Zr/CaO where y represents the amount in weight percent of Mg–Zr (Mg/Zr mass ratio of 2:1).

2.3. Catalyst characterization

Various characterization techniques were employed to examine the physicochemical properties of calcite powder and the synthesized catalysts. TGA analysis was performed to determine the final calcite decomposition temperature. This analysis was done using a Shimadzu TGA-50 apparatus (Model:TGA-50 Company: Shimadzu, Country: Japan) between 30 and 1000 °C with a temperature rise of 15 °C/min under airflow. XRD analysis was performed to investigate the morphology and crystal structure of the samples using a

Table 2
Physico-chemical properties of canola oil.

Property	Unit	Value
Saponification number	mgKOH/g	817
Acid number	mgKOH/g	0.072
Relative Density (20°C/water at 20°C)	g/cm^3	0.914–0.917
Kinematic viscosity (20°C)	mm^2/s	78.2
Smoke point	°C	220–230
Oleic acid	wt%	56
Linoleic acid	wt%	26
Linolenic acid	wt%	9
Palmitic acid	wt%	4
Stearic acid	wt%	2
Arachidic acid	wt%	2
other	wt%	1

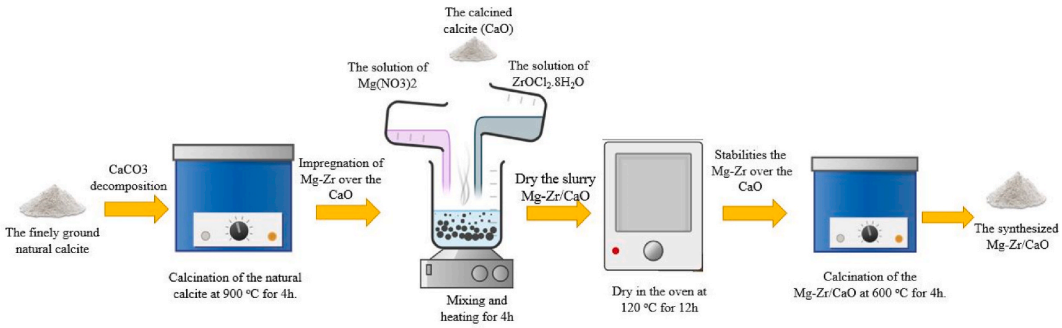

Fig. 1. The synthesis of the Mg–Zr/CaO via the wet impregnation method.

Bruker D8 X-ray (Model: D8, Company: Bruker, Country: Germany) diffractometer equipped with a Cu anode operating at 40 mA, 40 kV, and 2θ range between 0 and 80° with a step size of 0.026°. The specific surface area of the synthesized catalysts was determined by nitrogen physisorption at 77 K with a Quantachrome Autosorb 1 MP (Model: Autosorb 1 MP, Company: Quantachrome Country: USA) equipment using BET (Brunauer-Emmett-Teller) technique. Before analysis, the samples were degassed at 393 K overnight. SEM and EDX were performed using a SIGMA VP ZEISS apparatus (Model: SIGMA VP, Company: ZEISS, Country: Germany) operating at 10 kV. These analyses were performed to determine the distribution of the active phases on the support, morphology, elemental composition, and particle size. The basicity of the samples was determined using a titration method from the literature (Istadi et al., 2018).

2.4. Transesterification reaction

The transesterification reactions were carried out in a 100 ml 3-neck round bottom flask connected to a water-cooled condenser. A magnetic stirrer provided a mixing of the reactor content. The calcined catalyst was first activated by 30 min of mixing with methanol while heated at 40 °C. The required amount of oil was then added to the flask and the reaction was allowed to proceed at 60 °C for 3 h. The solid catalyst was recovered by centrifugation upon completion of the reaction. The remaining mixture was transferred to a separating funnel and left overnight for phase separation to be completed. The top layer was obtained as biodiesel while glycerol made up the bottom phase. The excess methanol in the biodiesel was removed by a rotary evaporator. In reusability tests, the spent catalyst was first separated using a centrifuge and subsequently washed with methanol to remove any adsorbed materials on the catalyst surface. The catalyst was then dried at 65°C for 12 h and subsequently calcined at 500°C for 3 h before being used in the next reaction cycle. All experimental tests for catalyst activity determination have been conducted three times to ensure the validity of obtained data. The FAME (fatty acids methyl ester) content was analysed using gas chromatography (Company: PerkinElmer, Model: Clarus 580, Country: USA) equipped with a flame ionization detector (FID) and a SUPRAWAX-280 capillary column (30 m, 0.25 mm ID, 0.25 μm). The carrier gas was Helium, and an internal standard was the diluted methyl nonadecanoate in hexane. The FAME content and conversation to FAME were determined using Equations (1) and (2), respectively (AlSharifi and Znad, 2019):

$$\mathrm{FAME}(\%) = \frac{\sum \mathrm{A\text{-}A_S}}{\mathrm{A_S}} \times \frac{\mathrm{C_S\ V_S}}{\mathrm{m}} \times 100\% \tag{1}$$

$$\mathrm{Conversion} = \frac{\sum \mathrm{A\text{-}A_S}}{\mathrm{A_S}} \times \frac{\mathrm{C_S\ V_S}}{\mathrm{m}} \times \frac{\text{mass of biodiesel}}{\text{mass of oil}} \times 100\% \tag{2}$$

where $\sum A$ is the summation of the areas under all peaks between $C_{4:0}$ and $C_{24:1}$, A_S is the peak area for methyl nonadecanoate, C_S is the concentration of methyl nonadecanoate solution (the internal standard), V_S is the volume of internal standard solution (ml), and m is the sample weight (mg). The synthesis steps are depicted in Fig. 2.

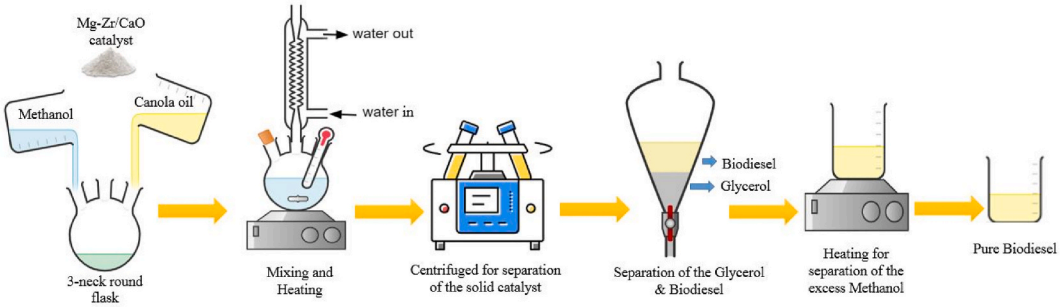

Fig. 2. The processes of the Transesterification Reaction.

3. Results and discussion

3.1. XRD analysis

The XRD patterns of fresh calcite, calcined calcite, and the synthesized catalysts are presented in Fig. 3, with a 2θ range between 5° and 80°. Calcium carbonate, which is the chemical formula of calcite, has three types of crystal phase structures called calcite, aragonite, and vaterite with the latter being unstable. The thermodynamically stable state of calcium carbonate under normal conditions is calcite. The XRD pattern for fresh calcite displays several peaks. The peak at 2θ = 36.18° corresponds to the Miller index [1 1 0], indicating the presence of the aragonite phase of calcium carbonate. Additionally, peaks are observed at 23.26°, 29.63°, 31.11°, 39.62°, 47.77°, 48.74°, 57.64°, 61.29°, and 65.92°, corresponding to the Miller indices [0 1 2], [1 0 4], [0 0 6], [1 1 3], [2 0 2], [0 1 8], [1 1 6], [1 2 2], [2 0 8], and [3 0 0], respectively. These peaks are indicative of the calcite phase of calcium carbonate.

Calcite was calcined at two different temperatures. It is known that only some of the calcite peaks would be removed at a calcination temperature of 800°C. At 900°C, however, all the peaks related to calcium carbonate had disappeared, and new peaks emerged at 2θ = 32.36°, 37.5°, 54°, 64.3°, and 67.5°, corresponding to the Miller indices [1 1 1], [2 0 0], [2 2 0], [3 1 1], and [2 2 2], respectively, indicating the presence of calcium oxide. The XRD patterns of the synthesized catalysts showed new peaks at 2θ = 43.14° and 62.5°, corresponding to the Miller indices [2 0 0] and [2 2 0], related to magnesium oxide, and at 2θ = 31.85°, corresponding to the Miller index [1 1 1], indicating the monoclinic phase of zirconium oxide. These peaks increased in intensity with increasing amounts of the active components (Kaur and Ali, 2014; Sree et al., 2009; Ngamcharussrivichai et al., 2010; Jalu et al., 2021; Gorban et al., 2022; Guilheiro et al., 2021; Rani et al., 2020; Yoosuk et al., 2010a).

3.2. SEM images

The SEM images of the calcite and the synthesized catalysts are illustrated in Fig. 4. Fresh calcite has low porosity before calcination (Fig. 4A). After calcination at high temperatures (Fig. 4B), the morphology had changed significantly leading to a more porous structure. This could be due to the release of carbon dioxide during the decomposition of calcium carbonate. The SEM results fully confirm the XRD findings, indicating that the fresh calcite exhibited large particles with smooth surfaces and a notably high degree of crystallinity. Upon calcination at 900 °C, these surfaces underwent significant changes, becoming rougher, and resulting in a reduction in particle size (Yoosuk et al., 2010b). Fig. 4C illustrates the dispersion of active components on the surface for the 7.5%Mg–Zr/CaO catalyst sample. In some places, the active component was clustered together to form larger particles that would reduce the porosity and surface area of the catalyst.

Results of EDX analysis for fresh calcite, calcined calcite, and 7.5% Mg–Zr/CaO catalyst are presented in Table 3 indicating that fresh calcite was composed of calcium, carbon, oxygen and small amounts of aluminium, silica, and magnesium as impurities. The

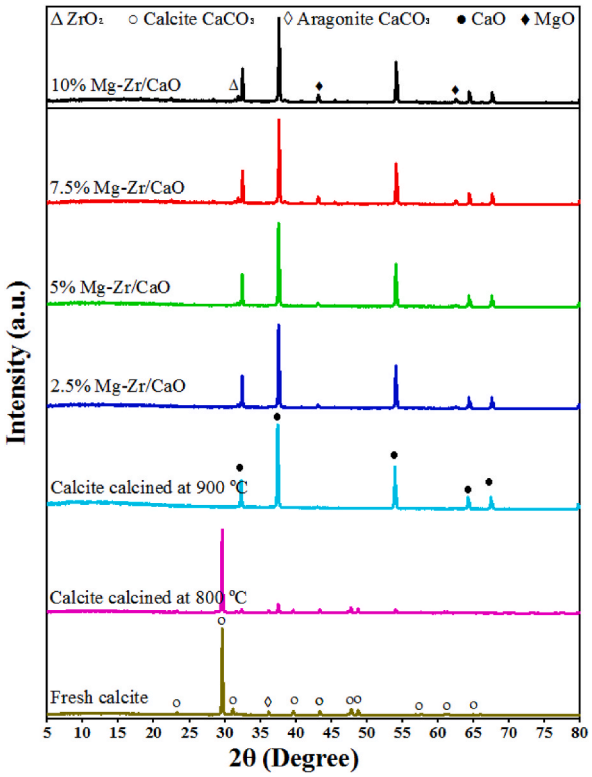

Fig. 3. XRD patterns of fresh calcite, calcined calcite, and synthesized catalysts.

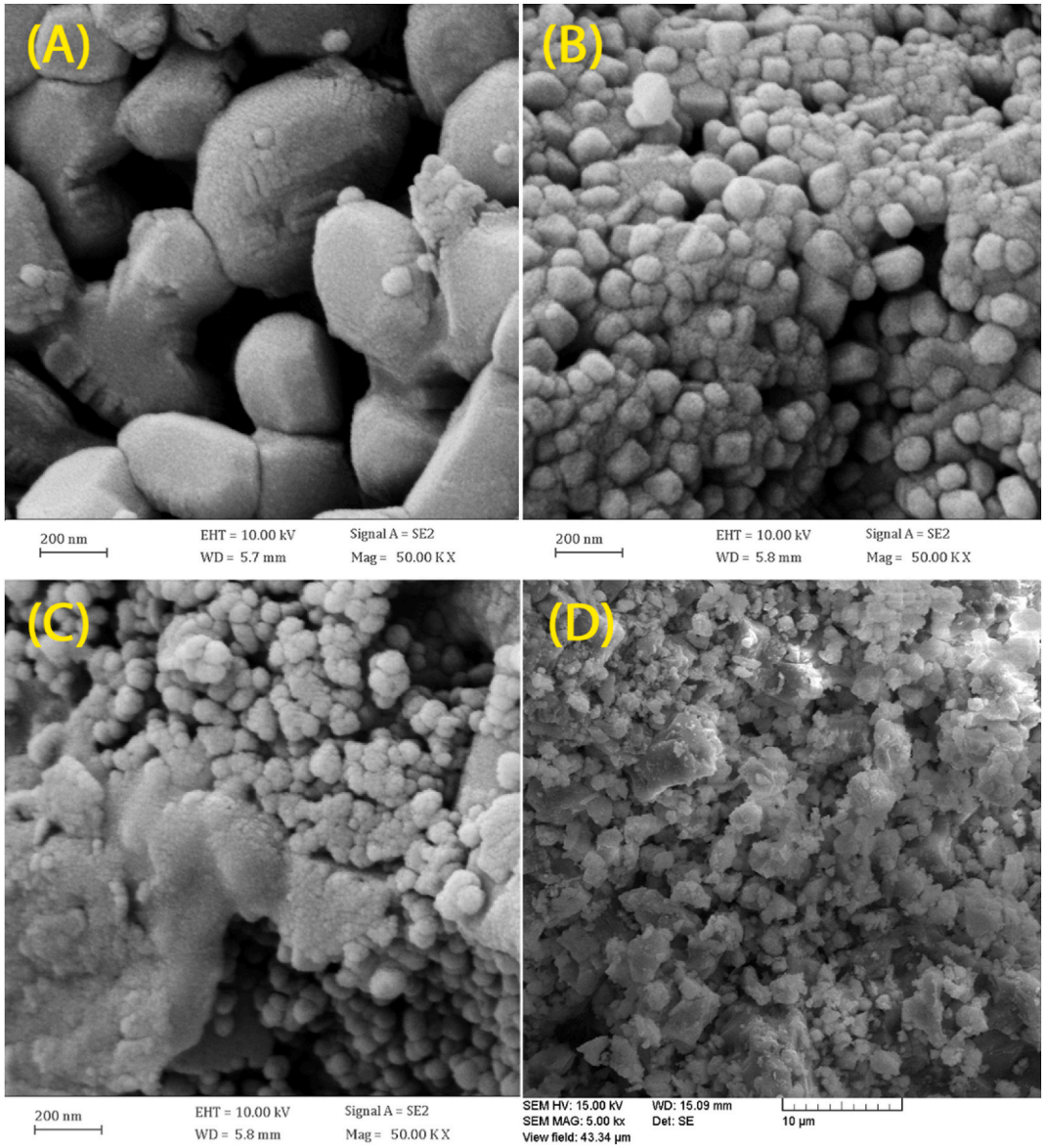

Fig. 4. SEM images of (A) fresh calcite, (B) calcined calcite, (C) fresh 7.5%Mg–Zr/CaO catalyst and (D) 7.5%Mg–Zr/CaO catalyst after four reaction cycles.

amount of carbon had decreased significantly with the release of CO_2 during calcination. The 7.5% Mg–Zr/CaO catalyst showed a slight increase in the weight percentage of magnesium in addition to zirconium atoms also being observed indicating a successful impregnation of active components on the calcined calcite. The weight ratio of Mg to Zr in this catalyst was close to the expected value.

3.3. TGA

Fig. 5 displays the TGA results for fresh calcite. The sample weight decreased by 52.3 wt% during the heating procedure where the temperature increased from 25 to 1000°C. The slight weight loss below 700 °C was a result of the moisture and organic materials

Table 3
EDX analysis of the fresh calcite, calcined calcite and 7.5% Mg–Zr/CaO catalyst.

Catalyst	Elemental content (wt%)						
	Ca	C	O	Si	Al	Mg	Zr
Fresh calcite	28.74	16.54	53.37	0.65	0.3	0.4	0
Calcined calcite	57.8	0.4	40.07	0.76	0.41	0.56	0
7.5% Mg–Zr/CaO	52.7	0.33	38.05	0.54	0.28	5.8	2.3

removal. Most of the weight loss occurred between 700 and 900 °C which was attributed to the release of carbon dioxide from the structure. After 900 °C, the sample weight remained almost constant indicating a complete decomposition. This result was consistent with the XRD analysis for calcined calcite at 900 °C and this temperature was, therefore, chosen as the maximum temperature for calcite calcination (Kouzu et al., 2008).

3.4. Catalyst basicity

The basicity of the synthesized catalysts was measured using a titration method (Table 4). First, the suspension of the catalyst sample (0.25 g) in benzene (10 ml of) was made, the colour of which was yellow. Then, bromothymol blue (32 mg) was solved in benzene (25 ml) to form a detector solution. By adding the detector solution to the suspension, the yellow colour of the suspension turned green-blue. The suspension was subsequently titrated by a 0.5 N benzoic acid solution to the point that the green colour completely disappeared. Basicity was determined according to Equation (3) where V, N, and W are the volume of benzoic acid solution (ml), the normality of benzoic acid solution (mgeq/ml) and the weight of the catalyst (g), respectively (Istadi et al., 2018; Khatibi et al., 2021).

$$\text{Basicity}\ (\text{mmol}/\text{g}) = \frac{(\text{V} \times \text{N})_{(\text{benzoic acid})}}{\text{W}_{\text{catalyst}}} \tag{3}$$

3.5. BET

Catalyst surface area is an important parameter affecting the catalytic activity. The adsorption and desorption isotherms for fresh calcite, calcined calcite, and the optimal catalyst (7.5% Mg–Zr/CaO) are presented in Fig. 6. All samples showed type IV isotherms that are related to the mesoporous structure of the material. The hysteresis loops for the samples were small and according to the IUPAC classification had properties similar to those of types H3 and H1. Fresh calcite indicated that the form of the hysteresis loop corresponded to type H3 for mesoporous fissures. The BET results indicated that calcination of calcite at 900 °C had changed the behaviour of the hysteresis loop from H3 to H1. The adsorption/desorption isotherms, however, did not change significantly after impregnation of the active component and subsequent calcination although the surface area and pore volume decreased (Yoosuk et al., 2010a).

BET results presented in Table 4 revealed the very small specific surface area of the natural calcite. Calcination at 900 °C altered not only the structural properties of calcite but also its chemical characteristics resulting in an increase in surface area and average pore diameter due to the release of carbon dioxide from carbonate-rich calcite. The surface area and average pore diameter for the synthesized catalysts decreased with increasing loading of the active components due to impregnation, and in some cases, sintering, of active components inside the pores thus blocking some of the pores.

3.6. Effect of active component loading

The canola oil transesterification reaction was carried out under the following experimental conditions: 5 wt% catalyst dosage, reaction temperature of 60 °C, methanol to oil ratio of 9:1, and reaction time of 3 h. The results are summarized in Table 5 indicating that almost no biodiesel was produced when fresh calcite was used. After calcination, however, the FAME content in the products had increased to 72.6% for the calcined calcite support. Impregnation of the calcined calcite with the active components led to an increase in the FAME content of the products with increasing active component loading with the maximum FAME content of 95.8% for the catalyst with active component loading of 7.5 wt%. An increase in active component loading beyond 7.5 wt% led to a slight decrease in the FAME content possibly due to pore blockage rendering the active sites inaccessible for the reactants (Chen et al., 2015a; AlSharifi and Znad, 2019). According to Table 5, Catalyst 7.5% Mg–Zr/CaO showed almost equal FAME yield compared to other catalysts reported at lower reaction temperatures, lower methanol to oil ratio and shorter time. This means reducing the cost, time, and energy consumption for biodiesel production.

3.7. Effect of catalyst dosage

To investigate the effect of catalyst dosage, the transesterification reactions were carried out at the reaction temperature of 60°C, the reaction time of 3 h, and the methanol to oil ratio of 9:1 using the 7.5% Mg–Zr/CaO catalyst at different dosages from 3 to 9 wt%. The results for these experiments are presented in Fig. 7. The FAME content in the products increased with increasing catalyst dosage

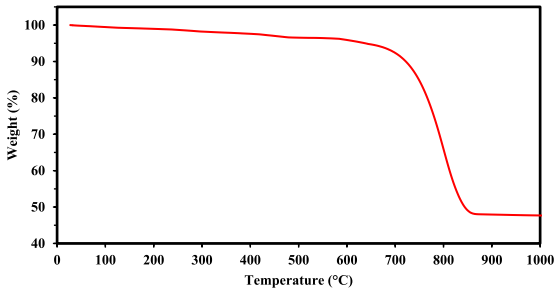

Fig. 5. TGA results for fresh calcite powder.

Table 4
Physical properties of fresh calcite and synthesized catalysts.

Catalyst	Total basicity (mmol/g)	Average pore diameter (nm)	Surface area (m^2/g)
Fresh calcite	2.6	11.02	0.65
Calcined calcite	7.5	63.79	11.5
2.5%Mg–Zr/CaO	8.1	34.31	10.8
5%Mg–Zr/CaO	9.3	27.1	9.7
7.5%Mg–Zr/CaO	11.5	22.6	8.4
10%Mg–Zr/CaO	11.1	15.3	7.2

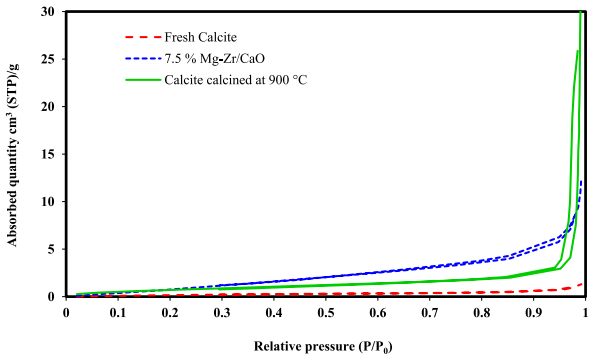

Fig. 6. (A) N_2 physisorption isotherms of the fresh calcite, calcined calcite and 7.5% Mg–Zr/CaO catalyst.

Table 5
Results of biodiesel production from transesterification of canola oil on different samples.

Catalyst	Catalyst loading (wt %)	Reaction time (h)	Methanol/oil molar ratio	Reaction temperature (°C)	FAME (%)	Ref.
Fresh calcite	5	3	9:1	60	2	This study
Calcined calcite	5	3	9:1	60	72.5	
2.5%Mg–Zr/CaO	5	3	9:1	60	81	
5%Mg–Zr/CaO	5	3	9:1	60	88	
7.5%Mg–Zr/CaO	5	3	9:1	60	95.8	
10%Mg–Zr/CaO	5	3	9:1	60	92.8	
KOH/ZSM-5-Fe_3O_4	9.03	3.26	12.3:1	65	93.65	
CaO/Talc	5	–	15:1	65	96.7	
Na–CaO/MgO	5	6	12:1	65	95.4	
CaO/sheep bone	5	5	12:1	60	95.18	
Hydrotalcite doped with $NaNO_3$	5	6	12:1	75	91	Reyes et al. (2014)

up to 7 wt%. Beyond this amount, however, the FAME content decreased slightly possibly due to the formation of a more viscous slurry inhibiting access of the reactants to the catalyst surface (Chen et al., 2014, 2015a).

3.8. Effect of methanol to oil molar ratio

Transesterification is a reversible reaction. In order to shift the equilibrium of the reaction towards the production of more biodiesel, the stoichiometric ratio of methanol to oil should be greater than 3:1. Excess methanol, on the other hand, complicates the separation process and also increases the cost of methanol recovery. To investigate the effect methanol to oil ratio, transesterification reactions were carried out with the 7.5%Mg–Zr/CaO catalyst at a dosage of 7 wt% at 60°C for 3 h using different molar ratios from 6:1 to 15:1. The results of these experiments are presented in Fig. 8 indicating that when the molar ratio of methanol to oil increased from 6:1 to 12:1, the FAME content in the products gradually increased to reach a maximum value. Further increase of the methanol/oil molar ratio beyond 12:1 led to a slight decrease in biodiesel production suggesting that the increase in the molar ratio of methanol/oil beyond the optimal value has reduced the relative concentration of the oil decreasing the forward reaction rate (Chen et al., 2015a; Teng et al., 2009).

3.9. Reusability

Reusability of the 7.5% Mg–Zr/CaO was investigated for consecutive reaction cycles at a catalyst dosage of 7 wt%, reaction temperature of 60 °C, methanol to oil ratio of 12:1, and reaction time of 3 h. The results (Fig. 9) indicate that the FAME contents in the product were 96.7, 91.3, 88.1, and 84% for the four consecutive cycles. The activity decrement after the end of each cycle can be

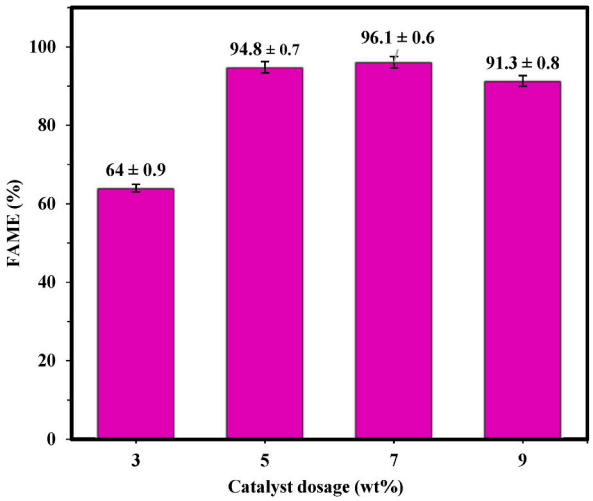

Fig. 7. Effect of catalyst dosage on the FAME content of products (methanol/oil ratio of 9:1, reaction temperature of 60 °C and 3 h s of reaction).

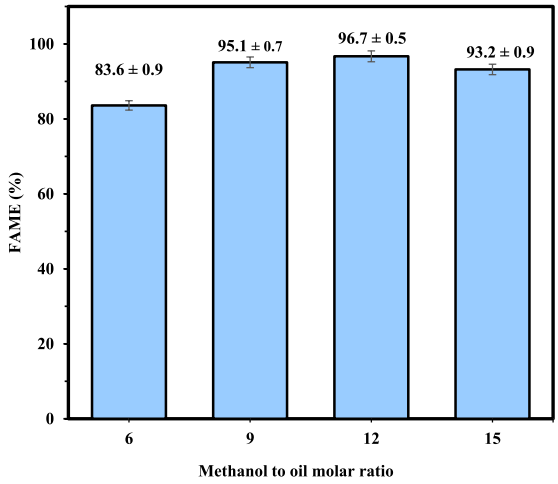

Fig. 8. Effect of methanol/oil molar ratio on the FAME content of products (7 wt% of catalyst, reaction temperature of 60 °C and 3 h of reaction).

attributed to the fouling of the surface-active sites by biodiesel and glycerol (Reaction products) or oil (unreacted feed) rendering them unavailable for the reactants. Fig. 4D shows the SEM image of catalyst 7.5% Mg–Zr/CaO after the fourth cycle. The figure shows that the catalytic particles have agglomerated in subsequent cycles and formed larger particles. This phenomenon has reduced the specific surface area and porosity, which has led to a decrease in FAME content production. Nevertheless, the FAME contents in the products obtained from recovered catalysts after consecutive cycles were high enough to indicate that the catalyst could be used for more than four cycles before losing its activity (Deng et al., 2011).

3.10. Product properties based on standards

Biodiesel prepared from canola oil transesterification reaction must have the characteristics of the EN 14214 and ASTM D6751 standards before usage in diesel engines. The physicochemical characteristics of biodiesel prepared under optimal conditions are shown in Table 6. According to Table 6, most of the obtained biodiesel properties comply with EN 14214 and ASTM D6751 standards. The cetane number is a measurement criterion used to determine the fuel combustion delay time, and the higher this number, the better the engine performance. In this study, the cetane number is higher than in other literature. Other characteristics, such as flash point and the presence of particles dissolved in the fuel, have demonstrated similar or superior results (Chen et al., 2015b; Ngamcharussrivichai et al., 2010).

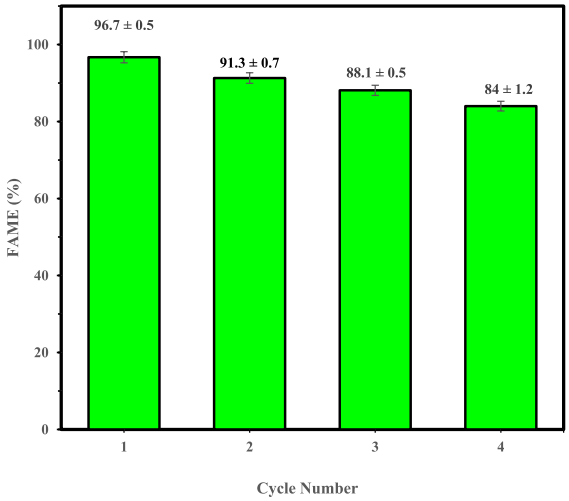

Fig. 9. Reusability of 7.5%Mg–Zr/CaO catalyst (7 wt% of catalyst, methanol/oil ratio of 12:1, 3 h of reaction and reaction temperature of 60 °C).

Table 6
Physical-chemical properties of biodiesel obtained under optimal conditions and using the 7.5%Mg–Zr/CaO catalyst.

Property	Unit	EN 14214	ASTM D6751	Prepared biodiesel
Kinematic viscosity (40 °*C*)	mm^2/s	3.50–5.00	1.9–6.0	3.57
Moisture content	wt.%	< 0.05	< 0.05	0.008
Density (15 °*C*)	Kg/m^3	860–900	860–894	882
Flash point	°*C*	> 120	> 120	146
Cetane number	–	> 51	> 47	54
Acid number	mg KOH/g	< 0.5	≤ 0.5	0.21
Oxidation stability (110 °*C*)	h	> 6	> 3	6.4
Glycerol	wt.%	< 0.02	< 0.02	0.012

4. Conclusions

The study focused on investigating the activity of calcium oxide derived from calcite and explored the influence of the Mg–Zr active phase, maintaining a Mg to Zr weight ratio of 2:1, in the transesterification process of canola oil with methanol for biodiesel production. Catalysts with varied loadings of the active phase (ranging from 2.5 to 10 wt%) were synthesized using the impregnation method, followed by calcination at 600 °C. Based on TGA analysis, the predominant weight reduction of natural calcite was observed within the temperature range of 700–900 °C, signifying the release of CO_2 from the calcite structure and the transformation of $CaCO_3$ into CaO through decomposition Among the catalysts tested, the 7.5% Mg–Zr/CaO catalyst demonstrated superior efficacy in biodiesel production. The catalyst's enhanced activity, compared to bare calcined calcite, can be attributed primarily to the improved basicity resulting from the impregnation with the active phase. By increasing the weight ratio of Mg–Zr doping to CaO, the total number of basic sites on the catalyst increased, reaching its maximum with the 7.5%(Mg–Zr)/CaO catalyst. Additionally, a similar variation pattern was observed for biodiesel production, indicating a direct relationship between the number of active basic sites and catalytic activity Optimal biodiesel yield, with a maximum FAME content of 96.7%, was achieved using the 7.5% Mg–Zr/CaO catalyst at a 7 wt % catalyst dosage, a methanol to oil molar ratio of 12:1, a reaction temperature of 60 °C, and a reaction time of 3 h. The stability and reusability of the catalyst were also assessed. After four consecutive cycles of utilizing the 7.5% Mg–Zr/CaO catalyst, the biodiesel yield dropped to 84%. This decline can be attributed to either the partial leaching of Mg and Zr into the reaction mixture or the blockage of active base sites by unreacted oil or the resulting product. This underscores the catalyst's reliability and its potential for practical application in biodiesel production processes. Biodiesel production via the transesterification reaction of canola oil with methanol has been reported with various catalysts. Catalyst 7.5% Mg–Zr/CaO demonstrated a FAME yield that was nearly identical to that of other catalysts, despite operating at lower reaction temperatures, lower methanol to oil ratios, and shorter reaction times. This implies that employing this catalyst could result in notable reductions in cost, time, and energy consumption for biodiesel production. For future work, it is possible to use a combination of acidic and basic active components, such as Mo–Li or W–Mg impregnation on natural calcite and measure the performance of these catalysts in biodiesel production from non-edible and waste oils.

CRediT authorship contribution statement

Morteza Talebi: Writing – original draft, Methodology, Investigation. **Afsanehsadat Larimi:** Software, Methodology,

Investigation, Formal analysis. **Farhad Khorasheh:** Validation, Supervision, Formal analysis. **Tohid N. Borhani:** Writing – review & editing, Project administration.

Declaration of competing interest

The authors declare that they have no known competing financial interests or personal relationships that could have appeared to influence the work reported in this paper.

Data availability

No data was used for the research described in the article.

References

Ahmadkhani, N., Haghighi, M., Taghavinezhad, P., 2019. Influence of MgO/CeO 2 ratio on CO 2 -oxidative transformation of C 2 H 6 to C 2 H 4 over highly active and stable Cr/MgO(x)–CeO 2 (100−x) nanocatalysts. Res. Chem. Intermed. 2 https://doi.org/10.1007/s11164-019-03782-8.

Akbari, E., Alavi, S.M., Rezaei, M., Larimi, A., 2022. Preparation and evaluation of A/BaO-MnOx catalysts (A: Rh, Pt, Pd, Ru) in lean methane catalytic combustion at low temperature. Int. J. Energy Res. 46, 6292–6313.

Ali, M.M., Ahmed, S.M.R., Aqar, D.Y., Gheni, S.A., Abdullah, G.H., Mahmood, M.A., Habeeb, O.A., Harvey, A., Phan, A.N., 2022. Use of dolomite catalyst in biodiesel production via transesterification of waste cooking oil in oscillatory baffled reactor. AIChE J. 68, e17751 https://doi.org/10.1002/aic.17751.

AlSharifi, M., Znad, H., 2019. Development of a lithium based chicken bone (Li-Cb) composite as an efficient catalyst for biodiesel production. Renew. Energy 136, 856–864.

Ba, J., Wei, G., Li, Z., Zhang, L., Pei, R., Xu, J., Zhou, Y., 2022. Castor oil transesterification catalyzed by a new red mud based LiAlO2-LiFeO2 composite. Energy Convers. Manag. 254, 115214 https://doi.org/10.1016/j.enconman.2022.115214.

Babatunde, E.O., Bamidele, S.H., Aderibigbe, F.A., Yusuff, A.S., Karmakar, B., Rokhum, S.L., Halder, G., 2022. Valorization of restaurant waste oil and cow-bone doped siliceous termite hills towards biodiesel production: kinetics and thermodynamics. Sustain Chem Pharm 30, 100895.

Boro, J., Konwar, L.J., Deka, D., 2014. Transesterification of non edible feedstock with lithium incorporated egg shell derived CaO for biodiesel production. Fuel Process. Technol. 122, 72–78.

Chen, G., Shan, R., Shi, J., Liu, C., Yan, B., 2015a. Biodiesel production from palm oil using active and stable K doped hydroxyapatite catalysts. Energy Convers. Manag. 98, 463–469.

Chen, G., Shan, R., Shi, J., Liu, C., Yan, B., 2015b. Biodiesel production from palm oil using active and stable K doped hydroxyapatite catalysts. Energy Convers. Manag. 98, 463–469. https://doi.org/10.1016/j.enconman.2015.04.012.

Chen, G., Shan, R., Shi, J., Yan, B., 2014. Ultrasonic-assisted production of biodiesel from transesterification of palm oil over ostrich eggshell-derived CaO catalysts. Bioresour. Technol. 171, 428–432.

Dahdah, E., Estephane, J., Taleb, Y., El Khoury, B., El Nakat, J., Aouad, S., 2021. The role of rehydration in enhancing the basic properties of Mg–Al hydrotalcites for biodiesel production. Sustain Chem Pharm 22, 100487.

de Lima, A.L., Ronconi, C.M., Mota, C.J.A., 2016. Heterogeneous basic catalysts for biodiesel production. Catal. Sci. Technol. 6, 2877–2891.

Dehkordi, A.M., Ghasemi, M., 2012. Transesterification of waste cooking oil to biodiesel using Ca and Zr mixed oxides as heterogeneous base catalysts. Fuel Process. Technol. 97, 45–51.

Deng, X., Fang, Z., Liu, Y., Yu, C.-L., 2011. Production of biodiesel from Jatropha oil catalyzed by nanosized solid basic catalyst. Energy 36, 777–784.

Devarajan, Y., Munuswamy, D.B., Subbiah, G., Vellaiyan, S., Nagappan, B., Varuvel, E.G., Thangaraja, J., 2022. Inedible oil feedstocks for biodiesel production: a review of production technologies and physicochemical properties. Sustain Chem Pharm 30, 100840. https://doi.org/10.1016/j.scp.2022.100840.

Elnasr, T.A.S., Al-Enezi, A.T., Hussein, M.F., Bielal, H., Alhumaimess, M.S., El-Ossaily, Y.A., Hassan, H.M.A., AlNahwa, L.H.M., Aldawsari, A.M., Alsohaimi, I.H., 2024. Sustainable biodiesel production from waste olive oil: utilizing olive pulp-derived catalysts for environmental and economic benefits. Sustain Chem Pharm 37, 101426.

Ezzatzadegan, L., Yusof, R., Morad, N.A., Shabanzadeh, P., Muda, N.S., Borhani, T.N., 2021. Experimental and artificial intelligence modelling study of oil palm trunk sap fermentation. Energies 14. https://doi.org/10.3390/en14082137.

Ghanei, R., Moradi, G., Heydarinasab, A., Seifkordi, A.A., Ardjmand, M., 2013. Utilization of constructional lime as heterogeneous catalyst in biodiesel production from waste frying oil. Int. J. Environ. Sci. Technol. 10, 847–854.

Gorban, O., Danilenko, I., Nosolev, I., Abdullayev, E., Islamov, A., Gavrilenko, K., Doroshkevich, O., Shvets, O., Kolotilov, S., 2022. Impact of chemical and physical modification of zirconia on structure, surface state, and catalytic activity in oxidation of α-tetralol. J. Nanoparticle Res. 24, 197. https://doi.org/10.1007/s11051-022-05566-5.

Guilheiro, J., Tatumi, S., Soares, A., Courrol, L., Barbosa, R.F., Rocca, R., 2021. Correlation study between OSL, TL and PL emissions of yellow calcite. J. Lumin. 233, 117881 https://doi.org/10.1016/j.jlumin.2020.117881.

Helwani, Z., Othman, M.R., Aziz, N., Kim, J., Fernando, W.J.N., 2009. Solid heterogeneous catalysts for transesterification of triglycerides with methanol: a review. Appl. Catal. Gen. 363, 1–10. https://doi.org/10.1016/j.apcata.2009.05.021.

Hu, M., Pu, J., Qian, E.W., Wang, H., 2023. Biodiesel production using MgO–CaO catalysts via transesterification of soybean oil: effect of MgO addition and insights of catalyst deactivation. Bioenergy Res 16, 2398–2410.

Istadi, I., Buchori, L., Putri, B.B.T., Hantara, H.I.A., 2018. Effect of Catalyst Pellet-Diameter and Basicity on Transesterification of Soybean Oil into Biodiesel Using K 2 O/CaO-ZnO Catalyst over Hybrid Catalytic-Plasma Reactor 06012, vols. 0–3.

Jairam, S., Kolar, P., Sharma-Shivappa Ratna, R., Osborne, J.A., Davis, J.P., 2012. KI-impregnated oyster shell as a solid catalyst for soybean oil transesterification. Bioresour. Technol. 104, 329–335. https://doi.org/10.1016/j.biortech.2011.10.039.

Jalu, R.G., Chamada, T.A., Kasirajan, DrR., 2021. Calcium oxide nanoparticles synthesis from hen eggshells for removal of lead (Pb(II)) from aqueous solution. Environ. Chall. 4, 100193 https://doi.org/10.1016/j.envc.2021.100193.

Kaur, M., Ali, A., 2011. Lithium ion impregnated calcium oxide as nano catalyst for the biodiesel production from karanja and jatropha oils. Renew. Energy 36, 2866–2871. https://doi.org/10.1016/j.renene.2011.04.014.

Kaur, N., Ali, A., 2014. Kinetics and reusability of Zr/CaO as heterogeneous catalyst for the ethanolysis and methanolysis of Jatropha crucas oil. Fuel Process. Technol. 119, 173–184.

Khatibi, M., Khorasheh, F., Larimi, A., 2021. Biodiesel production via transesterification of canola oil in the presence of Na–K doped CaO derived from calcined eggshell. Renew. Energy 163, 1626–1636.

Koh, M.Y., Ghazi, T.I.M., 2011. A review of biodiesel production from Jatropha curcas L. oil. Renew. Sustain. Energy Rev. 15, 2240–2251.

Kouzu, M., Kasuno, T., Tajika, M., Sugimoto, Y., Yamanaka, S., Hidaka, J., 2008. Calcium oxide as a solid base catalyst for transesterification of soybean oil and its application to biodiesel production. Fuel 87, 2798–2806. https://doi.org/10.1016/j.fuel.2007.10.019.

La Ore, M.S., Wijaya, K., Trisunaryanti, W., Saputri, W.D., Heraldy, E., Yuwana, N.W., Hariani, P.L., Budiman, A., Sudiono, S., 2020. The synthesis of SO4/ZrO2 and Zr/CaO catalysts via hydrothermal treatment and their application for conversion of low-grade coconut oil into biodiesel. J. Environ. Chem. Eng. 8, 104205.

Lam, M.K., Lee, K.T., Mohamed, A.R., 2010. Homogeneous, heterogeneous and enzymatic catalysis for transesterification of high free fatty acid oil (waste cooking oil) to biodiesel: a review. Biotechnol. Adv. 28, 500–518. https://doi.org/10.1016/j.biotechadv.2010.03.002.
Larimi, A.S., Alavi, S.M., 2012. Partial oxidation of methane over Ni/CeZrO2 mixed oxide solid solution catalysts. Int. J. Chem. Eng. Appl 3, 6–9.
Li, H., Niu, S., Lu, C., Liu, M., Huo, M., 2014. Transesterification catalyzed by industrial waste - lime mud doped with potassium fluoride and the kinetic calculation. Energy Convers. Manag. 86, 1110–1117. https://doi.org/10.1016/j.enconman.2014.06.082.
Li, Y., Lian, S., Tong, D., Song, R., Yang, W., Fan, Y., Qing, R., Hu, C., 2011. One-step production of biodiesel from Nannochloropsis sp. on solid base Mg-Zr catalyst. Appl. Energy 88, 3313–3317. https://doi.org/10.1016/j.apenergy.2010.12.057.
Mahesh, S.E., Ramanathan, A., Begum, K.M.M.S., Narayanan, A., 2015. Biodiesel production from waste cooking oil using KBr impregnated CaO as catalyst. Energy Convers. Manag. 91, 442–450.
Maleki, H., Kazemeini, M., Larimi, A.S., Khorasheh, F., 2017. Transesterification of canola oil and methanol by lithium impregnated CaO–La2O3 mixed oxide for biodiesel synthesis. J. Ind. Eng. Chem. 47, 399–404.
Moonsin, P., Roschat, W., Phewphong, S., Leelatam, T., Namwongsa, K., Thangthong, A., Panyakom, S., Yoosuk, B., Promarak, V., 2023. Modification of fresh-water clamshells (Pilsbryoconcha exilis compressa) as new raw material and its application in the biodiesel production of lard oil. Trends. Sci. 20, 6809.
Muciño, G.G., Romero, R., Ramírez, A., Martínez, S.L., Baeza-Jiménez, R., Natividad, R., 2014. Biodiesel production from used cooking oil and sea sand as heterogeneous catalyst. Fuel 138, 143–148. https://doi.org/10.1016/j.fuel.2014.07.053.
Nabgan, W., Jalil, A.A., Nabgan, B., Jadhav, A.H., Ikram, M., Ul-Hamid, A., Ali, M.W., Hassan, N.S., 2022. Sustainable biodiesel generation through catalytic transesterification of waste sources: a literature review and bibliometric survey. RSC Adv. 12, 1604–1627. https://doi.org/10.1039/D1RA07338A.
Ngamcharussrivichai, C., Nunthasanti, P., Tanachai, S., Bunyakiat, K., 2010. Biodiesel production through transesterification over natural calciums. Fuel Process. Technol. 91, 1409–1415. https://doi.org/10.1016/j.fuproc.2010.05.014.
Payapo, A.N.F., Utubira, Y., Sunarti, 2023. Modification of natural clay from Desa Luhu as heterogene catalyst in the transesterification of cooking oil into biodiesel. AIP Conf. Proc. 2642, 50002 https://doi.org/10.1063/5.0110633.
Phewphong, S., Roschat, W., Pholsupho, P., Moonsin, P., Promarak, V., Yoosuk, B., 2022. Biodiesel production process catalyzed by acid-treated golden apple snail shells (Pomacea canaliculata)-derived CaO as a high-performance and green catalyst. Eng. Technol. Appl. Sci. Res. 49.
Rani, N., Chahal, S., Kumar, P., Shukla, R., Singh, S., 2020. Role of oxygen vacancies for mediating ferromagnetic ordering in La-doped MgO nanoparticles. J. Supercond. Nov. Magnetism 33, 1–8. https://doi.org/10.1007/s10948-019-05374-4.
Reyes, I.C., Salmones, J., Zeifert, B., Contreras, J.L., Rojas, F., 2014. Transesterification of canola oil catalized by calcined Mg–Al hydrotalcite doped with nitratine. Chem. Eng. Sci. 119, 174–181.
Roschat, W., Butthichak, P., Daengdet, N., Phewphong, S., Kaewpuang, T., Moonsin, P., Yoosuk, B., Promarak, V., 2020. Kinetics study of biodiesel production at room temperature based on eggshell-dervied CaO as basic heterogeneous catalyst. Eng. Technol. Appl. Sci. Res. 47.
Roschat, W., Phewphong, S., Inthachai, S., Donpamee, K., Phudeetip, N., Leelatam, T., Moonsin, P., Katekaew, S., Namwongsa, K., Yoosuk, B., 2024. A highly efficient and cost-effective liquid biofuel for agricultural diesel engines from ternary blending of distilled Yang-Na (Dipterocarpus alatus) oil, waste cooking oil biodiesel, and petroleum diesel oil. Renew.Energy. Focus 48, 100540.
Roschat, W., Phewphong, S., Pholsupho, P., Namwongsa, K., Wongka, P., Moonsin, P., Yoosuk, B., Promarak, V., 2022. The synthesis of a high-quality biodiesel product derived from Krabok (Irvingia Malayana) seed oil as a new raw material of Thailand. Fuel 308, 122009.
Saikia, K., Moyon, N.S., Piloto-Rodríguez, R., Chai, F., Basumatary, S., Rokhum, S.L., 2023. Process optimization and kinetic studies of Musa glauca catalyzed biodiesel production. Sustain Chem Pharm 36, 101271.
Salaheldeen, M., Mariod, A.A., Aroua, M.K., Rahman, S.M.A., Soudagar, M.E.M., Fattah, I.M.R., 2021. Current state and perspectives on transesterification of triglycerides for biodiesel production. Catalysts. https://doi.org/10.3390/catal11091121.
Sharifzadeh, M., Sadeqzadeh, M., Guo, M., Borhani, T.N., Konda, N.V.S.N.M., Garcia, M.C., Wang, L., Hallett, J., Shah, N., 2019. The multi-scale challenges of biomass fast pyrolysis and bio-oil upgrading: review of the state of art and future research directions. Prog. Energy Combust. Sci. 71, 1–80. https://doi.org/10.1016/j.pecs.2018.10.006.
Soetaredjo, F.E., Ayucitra, A., Ismadji, S., Maukar, A.L., 2011. KOH/bentonite catalysts for transesterification of palm oil to biodiesel. Appl. Clay Sci. 53, 341–346. https://doi.org/10.1016/j.clay.2010.12.018.
Sree, R., Seshu Babu, N., Sai Prasad, P.S., Lingaiah, N., 2009. Transesterification of edible and non-edible oils over basic solid Mg/Zr catalysts. Fuel Process. Technol. 90, 152–157. https://doi.org/10.1016/j.fuproc.2008.08.008.
Sronsri, C., Sittipol, W., Kongpop, U., 2021. Performance of CaO catalyst prepared from magnetic-derived CaCO3 for biodiesel production. Fuel 304, 121419.
Suherman, S., Abdullah, I., Sabri, M., Silitonga, A.S., 2023. Evaluation of physicochemical properties composite biodiesel from waste cooking oil and schleichera oleosa oil. Energies 16, 5771.
Tahvildari, K., Anaraki, Y.N., Fazaeli, R., Mirpanji, S., Delrish, E., 2015. The study of CaO and MgO heterogenic nano-catalyst coupling on transesterification reaction efficacy in the production of biodiesel from recycled cooking oil. J Environ Health Sci Eng 13, 1–9.
Teng, G., Gao, L., Xiao, G., Liu, H., 2009. Transesterification of soybean oil to biodiesel over heterogeneous solid base catalyst. Energy Fuel. 23, 4630–4634. https://doi.org/10.1021/ef9003736.
Thakkar, K., Kachhwaha, S.S., Kodgire, P., 2022. A novel approach for improved in-situ biodiesel production process from gamma-irradiated castor seeds using synergistic ultrasound and microwave irradiation: process optimization and kinetic study. Ind. Crops Prod. 181, 114750.
Weldeslase, M.G., Benti, N.E., Desta, M.A., Mekonnen, Y.S., 2023. Maximizing biodiesel production from waste cooking oil with lime-based zinc-doped CaO using response surface methodology. Sci. Rep. 13, 4430. https://doi.org/10.1038/s41598-023-30961-w.
Widiarti, N., Ni'mah, Y.L., Bahruji, H., Prasetyoko, D., 2019. Development of CaO from natural calcite as a heterogeneous base catalyst in the formation of biodiesel: review. J. Renew. Mater. https://doi.org/10.32604/jrm.2019.07183.
Xia, S., Guo, X., Mao, D., Shi, Z., Wu, G., Lu, G., 2014. Biodiesel synthesis over the CaO–ZrO 2 solid base catalyst prepared by a urea–nitrate combustion method. RSC Adv. 4, 51688–51695.
Yan, B., Zhang, Y., Chen, G., Shan, R., Ma, W., Liu, C., 2016. The utilization of hydroxyapatite-supported CaO-CeO2catalyst for biodiesel production. Energy Convers. Manag. 130, 156–164. https://doi.org/10.1016/j.enconman.2016.10.052.
Yoosuk, B., Udomsap, P., Puttasawat, B., Krasae, P., 2010a. Modification of calcite by hydration–dehydration method for heterogeneous biodiesel production process: the effects of water on properties and activity. Chem. Eng. J. 162, 135–141.
Yoosuk, B., Udomsap, P., Puttasawat, B., Krasae, P., 2010b. Modification of calcite by hydration-dehydration method for heterogeneous biodiesel production process: the effects of water on properties and activity. Chem. Eng. J. 162, 135–141. https://doi.org/10.1016/j.cej.2010.05.013.
Yusuff, A.S., 2021. Parametric optimization of solvent extraction of Jatropha curcas seed oil using design of experiment and its quality characterization. S. Afr. J. Chem. Eng. 35, 60–68. https://doi.org/10.1016/j.sajce.2020.11.006.